

This is a repository copy of *The antimicrobial activity of a carbon monoxide releasing molecule (EBOR-CORM-1) is shaped by intraspecific variation within Pseudomonas aeruginosa populations.*

White Rose Research Online URL for this paper:
<http://eprints.whiterose.ac.uk/127017/>

Version: Accepted Version

Article:

Flanagan, Lindsey Anne, Steen, Rachel Rosemary, Saxby, Karinna Isobel et al. (7 more authors) (2018) The antimicrobial activity of a carbon monoxide releasing molecule (EBOR-CORM-1) is shaped by intraspecific variation within Pseudomonas aeruginosa populations. *Frontiers in Microbiology*. 195.

<https://doi.org/10.3389/fmicb.2018.00195>

Reuse

Items deposited in White Rose Research Online are protected by copyright, with all rights reserved unless indicated otherwise. They may be downloaded and/or printed for private study, or other acts as permitted by national copyright laws. The publisher or other rights holders may allow further reproduction and re-use of the full text version. This is indicated by the licence information on the White Rose Research Online record for the item.

Takedown

If you consider content in White Rose Research Online to be in breach of UK law, please notify us by emailing eprints@whiterose.ac.uk including the URL of the record and the reason for the withdrawal request.

1 **The antimicrobial activity of a carbon monoxide releasing molecule**
2 **(EBOR-CORM-1) is shaped by intraspecific variation within**
3 ***Pseudomonas aeruginosa* populations**

4 Lindsey Flanagan^{1,2}, Rachel Steen², Karinna Saxby^{1,2}, Mirre Klatter¹, Benjamin J.
5 Aucott², Craig Winstanley³, Ian J. S. Fairlamb², Jason M. Lynam², Alison Parkin² and
6 Ville-Petri Friman¹

7 ¹ The University of York, Department of Biology, Wentworth Way, York, YO10 5DD, UK

8 ² Department of Chemistry, University of York, Heslington, York, YO10 5DD, UK

9 ³ Department of Clinical Infection, Microbiology and Immunology, Institute of Infection and Global Health, Ronald Ross Building,
10 University of Liverpool, 8 West Derby Street, Liverpool, L69 7BE, UK

11 Correspondence: Ville-Petri Friman, The University of York, Department of Biology, Wentworth Way, York, YO10 5DD, UK, tel:
12 01904 328675, e-mail: ville.friman@york.ac.uk

13 **ABSTRACT**

14 Carbon monoxide releasing molecules (CORMs) have been suggested as a new synthetic
15 class of antimicrobials to treat bacterial infections. Here we utilised a novel EBOR-CORM-1
16 ([NEt₄][MnBr₂(CO)₄]) capable of water-triggered CO-release, and tested its efficacy against a
17 collection of clinical *Pseudomonas aeruginosa* strains that differ in infection-related
18 virulence traits. We found that while EBOR-CORM-1 was effective in clearing planktonic
19 and biofilm cells of *P. aeruginosa* strain PAO1 in a concentration dependent manner, this
20 effect was less clear and varied considerably between different *P. aeruginosa* cystic fibrosis
21 (CF) lung isolates. While a reduction in cell growth was observed after 8 hours of CORM
22 application, either no effect or even a slight increase in cell densities and the amount of
23 biofilm was observed after 24 hours. This variation could be partly explained by differences
24 in bacterial virulence traits: while CF isolates showed attenuated *in vivo* virulence and growth
25 compared to strain PAO1, they formed much more biofilm, which could have potentially
26 protected them from the CORM. Even though no clear therapeutic benefits against a subset of
27 isolates was observed in an *in vivo* wax moth acute infection model, EBOR-CORM-1 was
28 more efficient at reducing the growth of CF isolate co-culture populations harbouring
29 intraspecific variation, in comparison with efficacy against more uniform single isolate
30 culture populations. Together these results suggest that CORMs could be effective at
31 controlling genetically diverse *P. aeruginosa* populations typical for natural chronic CF
32 infections and that the potential benefits of some antibiotics might not be observed if tested
33 only against clonal bacterial populations.

34

35 **Keywords:** Biofilms, Carbon monoxide releasing molecules, CORM, Cystic fibrosis,
36 Polymicrobial infections, *Pseudomonas aeruginosa*, Synthetic chemistry, Virulence

37 1. INTRODUCTION

38 The rapid emergence of multidrug-resistant bacteria is a global problem that is predicted to
39 cause ten million deaths per year by 2050 (O'Neill, 2014). Antibiotic resistance often evolves
40 very quickly via *de novo* mutations and horizontal gene transfer (Normark and Normark,
41 2002), and as a result, antibiotic discovery has not been able to replace all of the antibiotics
42 that have now become ineffective (Brown and Wright, 2016). New methods and approaches
43 for treating bacterial infections are thus urgently required.

44 In recent years, carbon monoxide has emerged as a new potential therapeutic due to its
45 properties as a homeostatic and cytoprotective molecule with important signalling
46 capabilities (Motterlini and Otterbein, 2010). Carbon monoxide can be delivered via carbon
47 monoxide releasing molecules (CORMs), which are small molecules that release carbon
48 monoxide in response to certain environmental triggers such as enzymes (Stamellou et al.,
49 2014) or light (Jimenez et al., 2016). Nobre *et al.* first investigated the effect of CORMs on
50 bacteria (Nobre et al., 2007) and found that CORM-2 and CORM-3 reduced the number of
51 colony-forming units of *Escherichia coli* in minimal salts media and *Staphylococcus aureus*
52 in Luria Broth (LB) media (Nobre et al., 2007). The CORM effects were stronger in near-
53 anaerobic conditions and the activation of CORM required direct contact between the
54 molecule and its cellular targets (Nobre et al., 2007). Moreover, the effect of CORM-3 on
55 *Pseudomonas aeruginosa* wild type strain PAO1 was investigated by Desmard *et al.*
56 (Desmard et al., 2009), who found that treatment with the CORM reduced bacterial densities
57 and increased the survival of immunocompromised mice during an infection. It has also
58 previously been found that CORM-2 effectively reduces the densities of *P. aeruginosa*
59 planktonic and biofilm cultures with wild type and clinical strains (Murray et al., 2012).
60 Another study found that manganese-based Trypto-CORM is able to inhibit the growth of *E.*
61 *coli* when exposed to photochemical stimulus (Ward et al., 2014), while in the dark it is
62 active against *Neisseria gonorrhoeae* (Ward et al., 2017). In both cases, control experiments
63 indicate that the CO liberated from the metal is responsible for the observed behaviour.
64 However, most of the studies thus far have concentrated on exploring CORM effects on
65 relatively short time span (less than 24 hours). Furthermore, although it has been established
66 that many infections are polymicrobial, and that clinical bacterial pathogens can respond
67 differently to CORMs than laboratory strains, no studies have explored CORM effects on
68 bacterial co-cultures.

69 Cystic fibrosis (CF) is a genetically inherited disease which affects 1 in 2000 to 3000
70 newborn infants in the EU (who.int, 2010). Patients with CF often develop a thick mucus in
71 the lungs which they are unable to clear (Flume et al., 2010). This mucus makes patients
72 susceptible to frequent and recurring bacterial chest infections and the presence of *P.*
73 *aeruginosa* is often associated with increasing morbidity and loss of lung function (Pritt et
74 al., 2007). One of the key features of *P. aeruginosa* is its capability to rapidly adapt to the
75 lung environment and to become highly resistant to the antibiotics that are used to treat
76 infections (Smith et al., 2006;Poole, 2011;Folkesson et al., 2012;Winstanley et al., 2016). As
77 a result, *P. aeruginosa* populations show high levels of genetic variation within and between
78 CF patients (Marvig et al., 2013;Williams et al., 2015;O'Brien et al., 2017). This includes
79 phenotypic and genomic heterogeneity within genetically-related populations of *P.*
80 *aeruginosa* derived from the same clonal lineage (Mowat et al., 2011;Workentine et al.,
81 2013;Williams et al., 2015). This variation might also affect the applicability of potential
82 alternative therapies if it is linked with bacterial life-history traits that relate to potential
83 resistance mechanisms.

84 Here we synthesised and characterised a water-soluble CORM (EBOR-CORM-1),
85 $[\text{NEt}_4][\text{MnBr}_2(\text{CO})_4]$, and tested its effectiveness against *P. aeruginosa* strain PAO1 and a
86 selection of *P. aeruginosa* CF isolates originating from a single sputum sample from the
87 lungs of a CF patient, namely patient CF03 from previously published studies (Mowat et al.,
88 2011;Williams et al., 2015). Based on genome sequence data presented in a previous study,
89 these CF isolates were classified into two genetically distinct Liverpool Epidemic Strain
90 (LES) lineages, A and B (Williams et al., 2015;Williams et al., 2016), that differ regarding
91 their virulence traits (O'Brien et al., 2017). These genetically diverged lineages have been
92 shown to commonly coexist within individual patients and to share mutations via
93 homologous recombination that potentially help strains to adapt to the airway during chronic
94 infection (Williams et al., 2015). However, the implications of within-patient genetic
95 variation have been seldom considered in the context of antimicrobial therapies. We
96 hypothesised that effects of EBOR-CORM-1 could vary between different clinical isolates
97 and lineages, and that the susceptibility of isolates could be linked to expression of some
98 other bacterial virulence factors. We found that the CORM was effective in reducing both
99 planktonic and biofilm cells of strain PAO1 in a density-dependent manner. However,
100 CORM effects were more varied and generally weaker against clinical CF isolates.
101 Regardless, CORM efficiently reduced the growth of CF strain lineage co-cultures, which
102 suggest that CORMs could be effective at controlling genetically diverse *P. aeruginosa*
103 infections.

104 2. MATERIALS AND METHODS

105 ***Synthesis and properties of [NEt₄][MnBr₂(CO)₄], EBOR-CORM-1***

106 EBOR-CORM-1 was synthesised as described previously (Angelici, 1964): Mn(CO)₅Br (466
107 mg, 1.69 mmol) and 330 mg (1.57 mmol) of [(C₂H₆)₄N]Br were heated in 18 mL of absolute
108 methanol under a nitrogen atmosphere at 50 °C for 1 hour. The methanol was then
109 evaporated from the orange solution at the above temperature. The remaining yellow solid
110 was dissolved in 40 mL of chloroform, and the solution was filtered under nitrogen. After
111 adding 200 mL of hexane to the filtrate, the cloudy solution was allowed to stand under
112 nitrogen for 2 hours. The air-stable yellow crystals were separated by filtration, washed with
113 hexane, and dried under vacuum giving a yield of 88 % (636 mg). The compound was
114 characterised *via* solid state IR spectroscopy recorded using a KBr disk. Four main bands
115 were seen at 2090, 2001, 1984 and 1942 cm⁻¹ and a small shoulder was seen at 1897 cm⁻¹.
116 This is consistent with the literature values (Angelici, 1964). In a chloroform solution of
117 CORM four distinct bands were observed at 2092, 2015, 1987 and 1943 cm⁻¹, again this is
118 similar to previously reported literature values (Angelici, 1964). The change in the number of
119 carbonyl bands between the solid and solution phase measurements typically reflects that
120 different orientations are present in the solid state. The stability of the CORM in the solid
121 state was tested by heating a sample to 50 °C and running ATR IR spectra at 1 hour intervals.

122 Infrared detection of CO release from EBOR-CORM-1 following dissolution in different
123 solvents was conducted by dissolving 12 mg of CORM in 4 mL of solvent in a 25 mL round
124 bottomed flask attached to vacuum evacuated gas IR cell via a closed tap. After 1 h of stirring
125 the flask, the tap was opened to enable gas from the headspace of the flask to enter the IR
126 cell. Carbon monoxide could then be identified via the distinctive gaseous IR signature of a
127 double band, with fine rotational splitting, centred at 2150 cm⁻¹ (Klein et al., 2014). The
128 impact of different solvents can be quantified by comparison of the intensity of the CO bands
129 to those from CO₂, which is assumed to act as an effective internal standard.

130 The release of CO from EBOR-CORM-1 following dissolution in water was also followed via
131 solution phase monitoring of the metal complex's IR bands. In contrast to chloroform, when
132 EBOR-CORM-1 was first dissolved in water only two main IR bands were observed at 2050
133 and 1943 cm⁻¹. In order to investigate activity of EBOR-CORM-1 in liquid culture media, we
134 compared the effects of active and 'inactivated' CORM on the growth of PAO1 strain in LB
135 media as described previously (Murray et al., 2012). Briefly, CORM was inactivated by
136 storing a 2 mM CORM stock LB solution (10% v/v of standard LB concentration, i.e., the
137 same that was used in all the experiments; see below) at room temperature for 24 hours. To

138 estimate the effect of CORM inactivation on PAO1 growth, we added 50 μ L of freshly
139 prepared 2 mM CORM, 50 μ L of inactivated 2 mM CORM or 50 μ L 10% v/v LB (control) to
140 150 μ L of PAO1 starter culture on 96-well microplate. All treatments were replicated five
141 times and PAO1 growth monitored for 8 hours at 37 °C with spectrophotometer (OD 600 nm;
142 Tecan Infinite).

143 ***Bacterial strains and culture media***

144 In this study we used *P. aeruginosa* strain PAO1 (ATCC 15692), the earliest archived isolate
145 of the Liverpool Epidemic strain, LESB58 (Winstanley et al., 2009), and 19 clinical *P.*
146 *aeruginosa* LES isolates from the same sputum sample of a chronically infected CF patient
147 (Williams et al., 2015). The CF lung LES isolates originate from the sputum sample of one
148 patient, identified as patient CF03 in previous studies, and consist of two genetically separate
149 lineages A and B (Williams et al., 2015). Lineage A was represented by six isolates, namely
150 isolates: 2, 5, 10, 19, 23 and 25. Lineage B was represented by 13 isolates, namely isolates: 1,
151 6, 8, 17, 24, 26, 28, 32, 33, 34, 35, 36 and 37. Clinical isolates were collected with the
152 consent of the patient and under institutional human investigation approval. All strains and
153 isolates of *P. aeruginosa* were routinely cultured in liquid or solid LB media containing 10.0
154 g tryptone, 5.0 g yeast extract and 10.0 g NaCl in 1 L of ultra-pure water (final pH adjusted to
155 7.0 and 15 g of agar was used for solid media). For all experiments, starter cultures were
156 prepared from cryofrozen stocks by streaking frozen stock culture onto LB plates. After 24
157 hours growth, a single colony was selected and inoculated into 5 mL of liquid LB and grown
158 overnight in a shaking incubator at 37 °C in 50 mL centrifuge tubes. Overnight cultures were
159 centrifuged at 4000 rpm (11.5 g) for 15 min (Eppendorf), the resultant pellets were suspended
160 in 10% LB and bacterial densities adjusted to optical density at 600 nm of 0.066 before use
161 (OD 600nm), equalling $\sim 1 \times 10^8$ cells mL⁻¹.

162 ***Measuring the effects of EBOR-CORM-1 concentration on P. aeruginosa PAO1*** 163 ***strain***

164 We measured the effect of CORM concentration on *P. aeruginosa* PAO1 in four different
165 ways. First, we examined how EBOR-CORM-1 affects PAO1 growth after both 8 and 24
166 hours of inoculation in 10% LB media (bacteria and CORM inoculated at the same time).
167 Additionally, we measured how effective EBOR-CORM-1 is at clearing both established
168 planktonic and biofilm PAO1 cultures (bacteria pre-grown before adding EBOR-CORM-1).
169 All measurements were conducted on 96-well microplates and each treatment was replicated
170 5 times. A variety of EBOR-CORM-1 concentrations were tested by first preparing a 4 mM
171 CORM stock solution (dissolving EBOR-CORM-1 in 10% LB media by vortexing for 30 s

172 and sonicating for 1.5 min). The stock solution was then sterilised with syringe filtration and
173 serially diluted to result in 1 mM, 0.5 mM, 0.25 mM, 0.125 mM and 0 mM (control) EBOR-
174 CORM-1 concentrations and 1×10^8 PAO1 cells mL⁻¹ with final volume of 200 µl of media.
175 The microplate was then incubated at 37 °C for 24 hours.

176 All replicate populations were sampled at 8 and 24 hours after the start of the experiment (20
177 µl of samples) and serially diluted in sterile PBS on microplates to quantify the number of
178 living versus dead cells by flow cytometry. Briefly, DAPI (4',6-diamidino-2-phenylindole for
179 dead and living cells) and PI (Propidium iodide for dead cells) fluorescent stains (both from
180 Sigma-Aldrich) were added to microplate wells with diluted bacterial samples at
181 concentrations of 1 µg/mL and 50 µM, respectively. Plates were then incubated at room
182 temperature for 1 hour before measuring cell densities with a Cytoflex flow cytometer and
183 the CytExpert program. Every well was sampled for 60 s at fast speed setting. Gating of live
184 and dead cells was performed by monitoring DAPI staining on the PB450 channel with the
185 405 nm laser, and PI staining on the ECD channel of the 488 nm laser. Number of living cells
186 was determined as total cells (DAPI) – dead cells (PI).

187 To quantify the effects of EBOR-CORM-1 on established planktonic and biofilm cultures,
188 PAO1 was first grown in the absence of CORM at 37 °C for 48 hours. Cell cultures were then
189 inoculated with stock CORM solution to reach the same final concentrations as above: 1
190 mM, 0.5 mM, 0.25 mM, 0.125 mM and 0 mM (control) of CORM. The plate was incubated
191 for four more hours at 37 °C before sampling (20 µL), serial dilution and flow cytometry as
192 described above. To quantify effects of EBOR-CORM-1 on biofilm, crystal violet was added
193 to the remaining cell cultures at 10% v/v. After 15 min of incubation, the plate was rinsed
194 with deionised water and solubilised with 228 µL ethanol per well. The biofilm was
195 quantified by measuring absorbance at 600 nm.

196 ***Measuring the effects of EBOR-CORM-1 on clinical P. aeruginosa isolates in*** 197 ***mono- and co-cultures***

198 Similar to the PAO1 strain experiments, we measured the effect of EBOR-CORM-1 on
199 clinical *P. aeruginosa* isolates after 8 and 24 hours of inoculation in 10% LB media. We also
200 measured the impact of growing the isolates in the absence of EBOR-CORM-1 for 48 hours
201 and then applying EBOR-CORM-1 for 4 hours using both flow cytometry and crystal violet
202 staining. We used only one EBOR-CORM-1 concentration, 0.5 mM, which resulted in clear
203 reduction of PAO1 cultures (see results) alongside control treatment (no CORM).

204 In addition to measuring the effects of EBOR-CORM-1 in monocultures of each clinical
205 isolate, we also quantified the effect of the CORM on mixtures of the CF clinical isolates
206 from patient CF03. First, we prepared the clinical isolate starter cultures as described above,
207 then we mixed the standardised monocultures together in three different ways: as a whole
208 mix (all isolates mixed together in equal proportions), lineage A mix (all isolates classified as
209 lineage A mixed together in equal proportions) and lineage B mix (all isolates classified as
210 lineage B mixed together in equal proportions). All final mixes contained approximately $1 \times$
211 10^8 cells mL^{-1} before the application of 0.5 mM of EBOR-CORM-1. Each experiment was
212 replicated 5 times. After 24 hours growth at 37 °C, bacterial densities were measured by
213 using a Tecan infinite spectrophotometer: optical density measurements correlate well with
214 the proportion of living cells measured with flow cytometer (Supplementary figure 1).

215 ***Characterising bacterial virulence and growth***

216 To characterise production of the virulence factors pyocyanin and pyoverdine, all clinical
217 isolates were grown in 200 μL of 10% LB media in round-bottomed 96-well microplates for
218 48 hours at 37 °C (no shaking). After incubation, we measured the bacterial densities (OD
219 600 nm) and centrifuged the microplate for 10 min. at 4000 rpm (11.5 g) in a swing rotor
220 Eppendorf centrifuge. To measure pyocyanin and pyoverdine production, 150 μL of the
221 supernatant of each well was transferred to flat-bottomed 96-well microplates and the
222 absorbance spectrum measured with a spectrophotometer (Tecan infinite). Per capita
223 pyocyanin production was measured for each isolate by measuring the absorbance of
224 supernatant at 691 nm, and then standardizing by bacterial OD (Reszka et al., 2004). Per
225 capita production of the iron-chelating siderophore, pyoverdine, was measured by using
226 excitation-emission assay (O'Brien et al., 2017) where the fluorescence of each supernatant
227 well was measured at 470 nm following excitation at 380 nm, using a Tecan infinite M200
228 pro spectrophotometer. Also, OD was measured at 600 nm to quantify the ratio
229 fluorescence/OD as a quantitative measure of per capita pyoverdine production (O'Brien et
230 al., 2017). The isolate biofilm production was measured as described previously and growth
231 as maximum density and growth rate h^{-1} during 24-hour growth period. Lastly, we also
232 measured the *in vivo* virulence of each isolate by using wax moth model as described
233 previously (O'Brien et al., 2017).

234

235 ***Testing EBOR-CORM-1 antimicrobial activity in wax moth model in vivo***

236 To test the efficacy of EBOR-CORM-1 to constrain bacterial infections *in vivo*, we used a
237 wax moth larvae model (*Galleria mellonella* [Lepidoptera: Pyralidae], Livefood UK Ltd) and
238 followed the infection methodology described previously (O'Brien et al., 2017). We chose
239 three strains for infection experiments: PAO1, LESB58 and isolate 36 (Lineage B) from the
240 clinical sample collection. Before infection, we first grew the selected *P. aeruginosa* isolates
241 for 24 hours at 37 °C and subsequently diluted all cultures to approximately similar densities
242 (equalling approximately 1×10^6 cells mL⁻¹ in 0.8% w:v NaCl). The virulence of every
243 isolate was then tested in 16 independent wax moth larvae. We also infected 16 larvae with
244 0.8% w/v NaCl salt solution to control for the damage caused by the injection itself. The
245 larvae were injected with either 20 µL of one bacterial solution or NaCl buffer (“non-
246 infected”) between the abdominal segments six and seven with a 1 mL Terumo syringe. After
247 2 hours, 8 larvae from each bacterial infection or non-infection group were treated with 20
248 µL injection of 500 µM EBOR-CORM-1, and the other 8 were injected with 0.8% w:v NaCl
249 salt solution (control placebo) in the same location where the bacteria were originally
250 injected. After infection, larvae were placed on individual wells of 24-well cell culture plates
251 and the survival was monitored at 2-hour intervals for 3 days at 37 °C. Larvae were scored as
252 dead when they did not respond to touch with forceps. Larvae that were still alive after 7 days
253 from the infection were given a time of death of 168 hours. Every bacterial isolate was tested
254 for three times. It was concluded that the EBOR-CORM-1 injection alone did not affect
255 larval survival in the absence of bacteria (mortality similar between non-infected CORM-
256 injected larvae and non-infected CORM-free larvae: 5-10%).

257 **Statistical analysis**

258 All data were analysed with Generalized Mixed Models (factorial ANOVA) or regression
259 analysis where bacterial densities (Figs. 2, 3 and 4b) or trait values (Fig. 4a; Supplementary
260 figure 4) were explained with the presence and/or concentration of EBOR-CORM-1, CF
261 isolate identity (isolate number) or CF lineage (A or B). All proportional data (%) were
262 arcsine transformed before the analysis to meet the assumptions of parametric models.

263 **3. RESULTS**

264 **Chemistry of EBOR-CORM-1**

265 The stability of EBOR-CORM-1 in the solid state was demonstrated by heating a sample of
266 solid to 50 °C in air, and showing that there is very little difference in the carbonyl bands
267 observed in ATR IR spectra measured at 1 hour intervals over a 3-hour period (Fig. 1A). In
268 contrast, gas phase infrared analysis proved that CO release from EBOR-CORM-1 can be

269 triggered by dissolution in water, phosphate buffer or LB media, or addition of water to a
270 solution of the compound in an organic solvent (Fig. 1B).

271 Solution phase monitoring of the CO stretches of the compound showed that there was no
272 reaction with water over short periods of time, since dissolving EBOR-CORM-1 in water,
273 immediately re-drying it on a vacuum line and then re-dissolving the resultant solid in
274 chloroform yielded an IR spectra which matched that of the as-purified compound in
275 chloroform (Fig. 1C). The only two observed IR bands in the CORM spectrum in water
276 (2050 and 1943 cm^{-1}) were therefore attributed to the molecular symmetry of the hydrated
277 complex, rather than an immediate loss of CO upon contact with water. However, after 90
278 min in water, a loss of these carbonyl bands was observed, and this was attributed to the
279 release of all the CO from the complex (Fig. 1D).

280 ***EBOR-CORM-1 activity against planktonic and biofilm cells of P. aeruginosa*** 281 ***PAO1***

282 We found that applying EBOR-CORM-1 had generally negative effects on *P. aeruginosa*
283 PAO1 growth both after 8 and 24 hours of application ($F_{4, 25} = 50.9, p < 0.001$ and $F_{4, 25} =$
284 $31.8, p < 0.001$ for proportion of living cells after 8 and 24 hours, respectively, Fig. 2A) and
285 that these negative effects increased along with the increasing concentration of applied
286 EBOR-CORM-1 (regression analysis: $F_{1, 24} = 43, p < 0.001$ and $F_{1, 24} = 35, p < 0.001$ for
287 proportion of living cells after 8 and 24 hours, respectively, Fig. 2A). Similarly, EBOR-
288 CORM-1 was highly effective against both established planktonic and biofilm *P. aeruginosa*
289 PAO1 cultures ($F_{4, 25} = 77.5, p < 0.001$ and $F_{4, 25} = 39.5, p < 0.001$, respectively, Fig. 2A-B)
290 and the antimicrobial activity of CORM increased in a density-dependent manner (regression
291 analysis: $F_{1, 24} = 92, p < 0.001$ and $F_{1, 24} = 54, p < 0.001$, respectively, Fig. 2A-B).

292 ***EBOR-CORM-1 activity against planktonic and biofilm cells of clinical P.*** 293 ***aeruginosa cystic fibrosis isolates***

294 Similar to strain PAO1, we found that EBOR-CORM-1 had inhibitory effects on all tested
295 clinical *P. aeruginosa* isolates after 8 hours of application of CORM ($F_{1, 152} = 11969, p <$
296 0.001 , Fig. 3A). While this effect did not depend on the lineage (CORM \times lineage: $F_{1, 152} =$
297 $1.4, p < 0.001$), it varied between different clinical isolates (CORM \times isolate: $F_{18, 152} = 11969,$
298 $p < 0.001$, Fig. 3A). In contrast, EBOR-CORM-1 had slightly positive effects on *P.*
299 *aeruginosa* growth after 24 hours of application ($F_{1, 152} = 256, p < 0.001$, Fig. 3B) and this
300 effect varied between different isolates (CORM \times strain: $F_{18, 152} = 2.8, p = 0.001$) being
301 slightly stronger (i.e. positive) with isolates belonging to a lineage B (CORM \times lineage: $F_{1,$

302 $_{152} = 24.9, p < 0.001$, Fig. 3B). EBOR-CORM-1 also had negative effects when applied to
303 established *P. aeruginosa* cell cultures ($F_{1, 152} = 222, p < 0.001$, Fig. 3C). However, these
304 effects depended on the isolate (CORM \times isolate: $F_{18, 152} = 2.8, p = 0.001$) and the lineage
305 ($F_{1, 152} = 65.2, p = 0.001$), reduction being relatively larger with isolates belonging to lineage
306 A (Fig. 3C). In the case of established biofilms, EBOR-CORM-1 had a slightly positive
307 effect ($F_{1, 152} = 9.6, p = 0.002$, Fig. 3D) and while this effect varied between different isolates
308 ($F_{18, 152} = 2.0, p = 0.01$) it did not differ between the lineages ($F_{1, 152} = 1.2, p = 0.265$,
309 respectively, Fig. 3D). Together these results suggest that compared to strain PAO1, EBOR-
310 CORM-1 effects varied more with the clinical *P. aeruginosa* isolates having negative, neutral
311 or positive effects on bacterial growth depending on the isolate identity, lineage and the
312 timing of CORM application.

313 **Linking EBOR-CORM-1 antimicrobial activity with clinical *P. aeruginosa* isolate** 314 **virulence and growth**

315 We found that all the isolates belonging to a lineage A formed non-mucoid colonies (6 out of
316 6), while most of the isolates belonging to a lineage B formed mucoid (i.e., mucus-like)
317 colonies (11 out of 13) on LB plates (typical mucoid and non-mucoid colonies shown in
318 supplementary figure 3). All clinical isolates differed from the non-mucoid PAO1 strain
319 respective of their virulence and growth (Fig. 4A). More specifically, clinical isolates
320 produced less pyoverdine ($F_{1, 23} = 286, p < 0.001$) and pyocyanin ($F_{1, 23} = 170, p < 0.001$) and
321 grew slower ($F_{1, 23} = 91, p < 0.00$) and reached lower maximum densities in LB medium ($F_{1,$
322 $_{23} = 15.5, p = 0.001$, Fig. 4A). However, clinical isolates produced a considerably larger
323 amount of biofilm ($F_{1, 23} = 21.7, p < 0.001$) and showed very low virulence (high time to
324 death) in wax moth larvae *in vivo* ($F_{1, 23} = 1296, p < 0.001$, Fig. 4A).

325 When comparing the two CF lineages, we found that isolates belonging to a lineage B
326 consistently outperformed the isolates belonging to a lineage A by producing more
327 pyoverdine ($F_{1, 18} = 6.06, p = 0.025$), biofilm ($F_{1, 18} = 15.08, p = 0.001$) and by growing faster
328 ($F_{1, 18} = 22.35, p < 0.001$) and to higher maximum densities ($F_{1, 18} = 6.27, p = 0.023$) in LB
329 medium (Fig. 4A; Supplementary figure 4). However, lineages did not differ in pyocyanin
330 production ($F_{1, 18} = 1.99, p = 0.176$) or virulence ($F_{1, 18} = 1.03, p = 0.324$; Fig. 4A;
331 Supplementary figure 4). Across all clinical isolates, density reduction by CORM correlated
332 negatively with biofilm formation ($F_{1, 18} = 4.8, p = 0.042$). Together these results suggest that
333 clinical isolates differed from PAO1 and from each other respective to various life-history
334 traits important for establishing an infection.

335 **EBOR-CORM-1 activity against clinical *P. aeruginosa* CF isolate co-cultures**

336 Despite the observed isolate-specific variation in *P. aeruginosa* monocultures, EBOR-
337 CORM-1 was effective in reducing the growth of *P. aeruginosa* co-cultures after 24 hours of
338 application (CORM: $F_{1, 24} = 132$, $p < 0.001$, Fig. 4B). Moreover, this reduction was the same
339 regardless of whether the mix contained only one lineage or both lineages (CORM \times co-
340 culture: $F_{2, 24} = 0.5$, $p = 0.612$). These results suggest that intraspecific *P. aeruginosa*
341 population heterogeneity makes the bacteria more susceptible to EBOR-CORM-1 treatment.

342 **EBOR-CORM-1 activity against *P. aeruginosa* strains in wax moth model**

343 We found that *P. aeruginosa* isolates differed in their virulence (time to death) from each
344 other ($F_{2, 24} = 12.2$, $p < 0.001$): PAO1 and LESB58 strains were equally virulent, and both
345 exhibited higher virulence than the clinical isolate 36 (killing larvae approximately in 17
346 hours [PAO1], 36 hours [LESB58] and 92 hours [clinical isolate 36]; values averaged over
347 both non-CORM and CORM treatments, Fig. 5). In contrast to *in vitro* results, application of
348 EBOR-CORM-1 did not increase the survival of infected larvae ($F_{1, 24} = 1.3$, $p = 0.257$) with
349 any of the infected strains (CORM \times strain: $F_{2, 24} = 1.4$, $p = 0.273$, Fig. 5). All larvae became
350 highly pigmented (black throughout) during the infection regardless of the *P. aeruginosa*
351 isolate.

352 **4. DISCUSSION**

353 Here we set out to study the antimicrobial activity of [NEt₄][MnBr₂(CO)₄], EBOR-CORM-1,
354 against clinical *P. aeruginosa* isolates *in vitro*. This CORM was chosen as a suitable
355 representative of this class of molecule based on the aqueous solubility, facile synthesis
356 (Angelici, 1964), content of a non-toxic metal core, and simple architecture which makes it
357 akin to a “parent compound” for CORMs that have been engineered to possess sophisticated
358 CO release mechanisms. In contrast to more complex CORMs, the molecule was shown to
359 have a water activated mechanism of CO release, as seen in previous studies of [MX(CO)₅]
360 species, where X is a halide (Zhang et al., 2009). Such water induced degradations are
361 believed to proceed via a two-step pathway whereby water causes loss of the halide followed
362 by formation of a dimer species; from which the CO is released. This may explain the
363 changes in the IR spectra recorded in water when compared to chloroform, although the data
364 do not directly match those for [Mn₂Br₂(CO)₈] (El-Sayed and Kaesz, 1963), the product
365 expect on loss of Br⁻ from EBOR-CORM-1. We found that while EBOR-CORM-1 showed
366 density-dependent antimicrobial activity against both planktonic and biofilm cells of the
367 widely studied laboratory-adapted strain PAO1, these effects were more varied and weaker
368 against clinical CF lung isolates. Regardless, EBOR-CORM-1 was efficient at reducing the

369 growth of CF isolate lineage mixes, which suggests that it could have therapeutic potential in
370 controlling heterogeneous *P. aeruginosa* infections. Solutions of inactivated EBOR-CORM-1
371 were essentially inactive against *P. aeruginosa* strain PAO1 (Supplementary figure 2)
372 implying that, at least in this case, the observed activity was due to CO released from the
373 complex rather than the residual metal salts (or indeed $[\text{NEt}_4]^+$).

374 Similar to a study published by Murray *et al.* (2012), we found considerable variation in
375 CORM antimicrobial activity between different clinical CF isolates, which depended whether
376 we explored EBOR-CORM-1 effects on relatively short (8 hours) or long timescales (24
377 hours) and if we compared CORM antimicrobial activity on actively growing and established
378 cell cultures (after 48 hours of bacterial growth). Our results after 8 hours of EBOR-CORM-1
379 application are very similar to a previous study (Murray *et al.*, 2012) showing clear reduction
380 in bacterial densities. However, this effect vanished by the 24 hour time point, and
381 surprisingly, some bacterial isolate cultures reached higher optical densities in the presence
382 compared to absence of CORM, which could have been due to increase in number of cells or
383 expression of exoproducts that were picked up by OD600 nm (e.g. pyocyanin or alginate).
384 The most likely explanation for this is that CORM effects were short-lived (Fig. 1), which
385 allowed bacteria to recover and grow to high densities during 24 hours after application of
386 CORM. However, when CORM effects were measured after 4 hours of application to
387 established cell cultures, we could still observe clear reduction in mean bacterial densities.
388 Together these results suggest that CORM effects could be seen up to 4 hours post
389 application and that CORM could eradicate bacterial cells whether they are at exponential or
390 stationary phase of their growth. Interestingly, CORM effects varied between clinical isolates
391 and were clearer with the isolates belonging to lineage A. While Murray *et al.* (2012) did not
392 observe clear variation in CORM effects against planktonic cell cultures, they found
393 differences in CORM efficiency in eradicating bacterial biofilms. This is also consistent with
394 our data and reinforces the hypothesis that *P. aeruginosa* clinical isolates are likely to
395 respond differently to CORM therapies.

396 To explore clinical isolate variation in more detail, we compared differences in bacterial
397 virulence and growth traits between the PAO1 and clinical CF lung isolates. We found that
398 relative to strain PAO1, clinical CF isolates grew slower, had lowered virulence and
399 produced lower amounts of pyoverdine and pyocyanin, which are important virulence factors
400 (O'Brien *et al.*, 2017). This is consistent with previous research and typical for *P. aeruginosa*
401 isolates retrieved from chronic lung infections (Smith *et al.*, 2006;Folkesson *et al.*,
402 2012;Marvig *et al.*, 2013;Williams *et al.*, 2015). The clinical isolates produced much more

403 biofilm compared to strain PAO1 and biofilm formation was the highest in the isolates
404 belonging to lineage B. Biofilms could potentially provide a protective function against
405 CORMs. Biofilms often have much higher antibiotic resistance than their aquatic
406 counterparts (Stewart and William Costerton, 2001) and there are multiple reasons for this.
407 First, antibiotics might be ineffective because the biofilm acts as a diffusion barrier (de Beer
408 et al., 1997). Second, subpopulations within the biofilm can sometimes differentiate into a
409 highly protected phenotypes that can repopulate the biofilms (Cochran et al., 2000). Third,
410 the biofilm might change the chemical microenvironment, forming zones of nutrient and
411 oxygen depletion or waste accumulation that prevents the antibiotics from functioning
412 optimally (de Beer et al., 1994). Although we did not explore this specifically, clinical
413 isolates belonging to a lineage A were more susceptible to CORMs and produced relatively
414 less biofilm compared to strains belonging to a lineage B. Thus, overall a negative correlation
415 was found between density reduction by CORM and biofilm formation. Our results therefore
416 suggest that biofilm might provide a protective function against the CORM.

417 Despite the isolate variations observed in bacterial monocultures, EBOR-CORM-1 was
418 effective at reducing the growth of *P. aeruginosa* clinical isolate mixed cultures. One
419 explanation for this is that, in addition to CORM, *P. aeruginosa* growth was limited by
420 antagonistic intraspecific species interactions in co-cultures. *P. aeruginosa* has been shown to
421 exert both facilitative and antagonistic effects on each other via siderophore (Harrison et al.,
422 2008) and bacteriocin (Ghoul et al., 2015) production. In our case, all the clinical isolates
423 were derived from the same Liverpool Epidemic Strain clonal lineage and therefore likely
424 carried the same siderophore and bacteriocin genes. Additionally, resource competition is
425 likely to further limit *P. aeruginosa* growth both in CF lungs and simplified laboratory
426 microcosms. As a result, even though some clinical strains were relatively insensitive to
427 EBOR-CORM-1, their growth could have been constrained by competition with the other
428 strains in co-cultures. We found that this was the case for all strain mixes regardless if the
429 strains belonged to a lineage A, B or them both. This suggests that the susceptibility of the
430 lineages measured in monocultures did not predict the susceptibility of isolate mixes within
431 or between lineages. However, such antagonism was not observed in the absence of EBOR-
432 CORM-1, which suggests that CORM-triggered antagonistic intraspecific interactions in *P.*
433 *aeruginosa* co-cultures. Mechanistically, this could have been driven by competition sensing
434 in response to CORM-mediated cell damage in *P. aeruginosa* populations (Cornforth and
435 Foster, 2013). However, this needs to be confirmed in future experiments. Interestingly, all
436 the clinical strains we used originated from a single CF patient and interactions between them
437 thus reflect the realistic ecology of CF lungs. In the future, it would be useful to determine

438 pairwise interactions between these CF strains and look at CORM effects on other coexisting
439 bacterial species observed in CF infections (Folkesson et al., 2012).

440 We found that EBOR-CORM-1 had no clear therapeutic benefits in the wax moth infection
441 model. There are several potential explanations for this. First, EBOR-CORM-1 had limited
442 long-term activity when in contact with water. As a result, the bactericidal effect may only
443 have elicited lag in the initial phase of bacterial growth and proliferation within the wax
444 moths. Second, insect tissue is not homogeneous and it is possible that we failed to deliver
445 the CORM to the specific area of infection, or that bacteria were able to colonise new areas
446 that were not exposed to the CORM. Third, insects differ from laboratory media (such as LB)
447 as a bacterial growth environment, which could also affect pathogen virulence. For example,
448 it has been recently demonstrated that plant versus animal based growth media can have
449 physiological effects on bacterial virulence (Ketola et al., 2016) and that LB media does not
450 adequately reflect *P. aeruginosa* growth on lung tissue (Harrison et al., 2014; Harrison and
451 Diggle, 2016). Hence, the wax moth injection model might not reliably reflect the virulence
452 of CF isolates derived from chronic infections. However, it is also the case that many of the
453 affordable and available CF infection animal models do not truly reflect the real CF lung
454 disease environment. It remains to be established whether CORM therapy could be applied in
455 the context of CF lung infections. It is possible, for example, that it might be more suitable
456 for treating topical infections such as burn wounds, for which better animal models are
457 available (Rumbaugh et al., 2012).

458 Further work is also needed to understand the mode of action of EBOR-CORM-1. While
459 respiratory oxidases and globins at heme targets are generally considered the prime targets of
460 CO and CORMs (Wareham et al., 2015), it has been demonstrated that CORMs can have
461 multiple different other targets (Wilson et al., 2015). For example, CO also binds to the di-
462 iron site in bacterial NO reductases and to iron, copper, and nickel sites in certain microbial
463 proteins such as CO dehydrogenase (Lu et al., 2004; Wasser et al., 2005). In some cases,
464 CORMs might have intracellular targets but their accumulation within the cells can be very
465 weak (Tinajero-Trejo et al., 2016). Moreover, in the future it would be important to test if
466 EBOR-CORM-1 is cytotoxic to eukaryotic cells. The concentration we used are in line with
467 previously published work where no, or very mild, cytotoxic effects were observed (Murray
468 et al., 2012). We are currently conducting experiments to validate this independently and to
469 understand how EBOR-CORM-1 interacts with bacterial cells. While, our wax moth assays
470 show that the concentrations we used had no negative effects on short-term insect viability,
471 more detailed cytotoxicity assays are needed in the future. Lastly, the low solubility of

472 EBOR-CORM-1 in water, and its activation in this medium, is problematic for delivery and
473 activation at specific sites within patients. In addition to chemically increasing the molecule
474 stability, CORMs could be enclosed in microvesicles (van Dommelen et al., 2012) to ensure
475 more efficient antimicrobial activity and drug delivery.

476 In conclusion, our results show that EBOR-CORM-1 shows antimicrobial activity against
477 both planktonic and biofilm cells of *P. aeruginosa* strain PAO1 but that these effects are
478 more varied and less pronounced against clinical CF lung isolates in monocultures. In
479 contrast, more heterogeneous *P. aeruginosa* populations comprising intraspecific phenotypic
480 variants were more susceptible to CORM treatment. This potentially has wider implications
481 in the testing of novel therapeutics. At present, this is done almost exclusively using clonal *P.*
482 *aeruginosa* populations. Our observations suggest that testing carried out on more
483 heterogeneous populations of *P. aeruginosa*, more closely resembling those found in the CF
484 lung, may give different and sometimes more promising results.

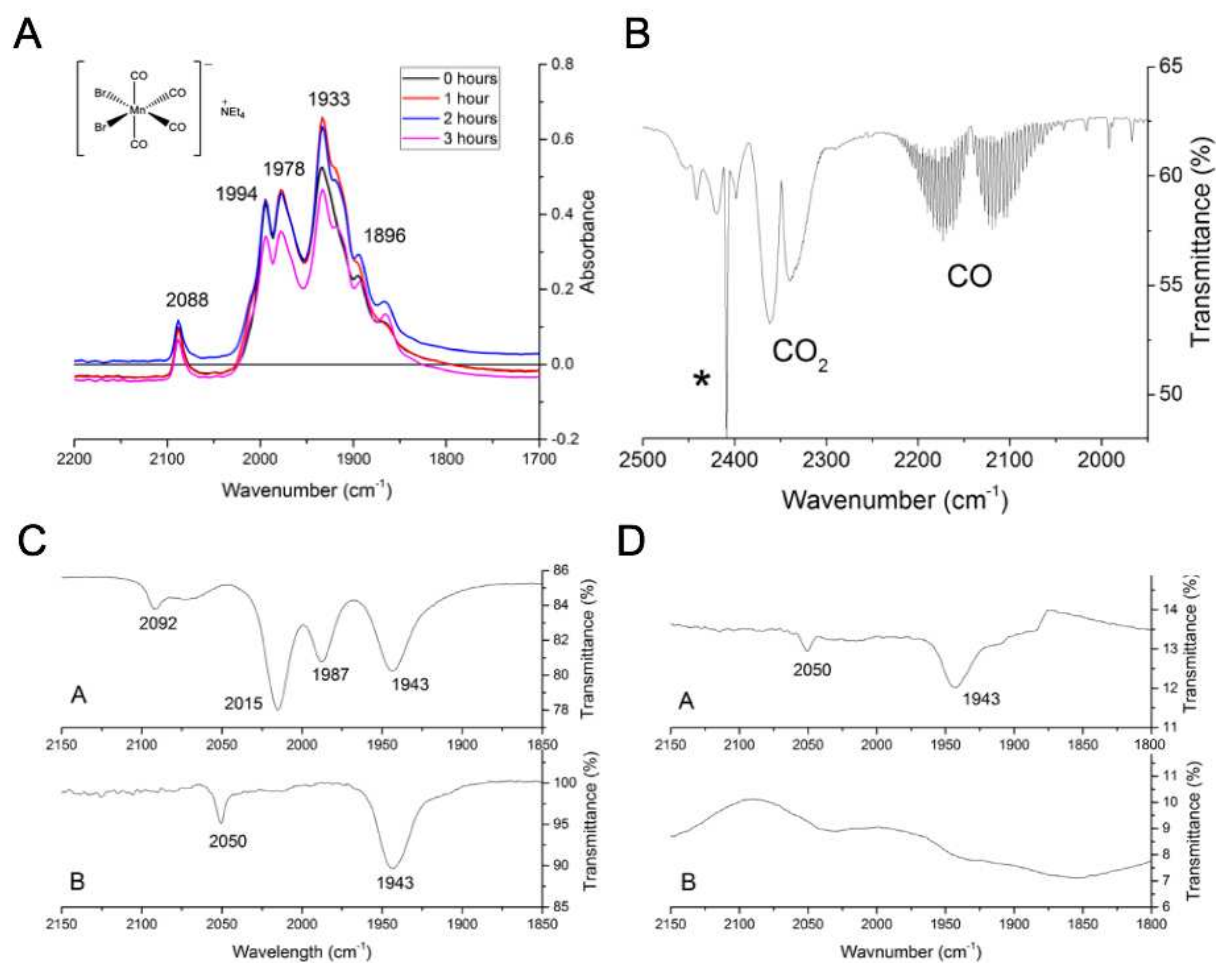
485

486 **ACKNOWLEDGEMENTS**

487 We thank James Pitt for carrying out an initial EBOR-CORM-1 synthesis and TARGeTED
488 Antimicrobial Resistance (AMR) Project and EPSRC council for funding (EP/M027538/1).
489 Ville-Petri Friman is also supported by the Wellcome Trust [reference no. 105624] through
490 the Centre for Chronic Diseases and Disorders (C2D2) at the University of York.

491

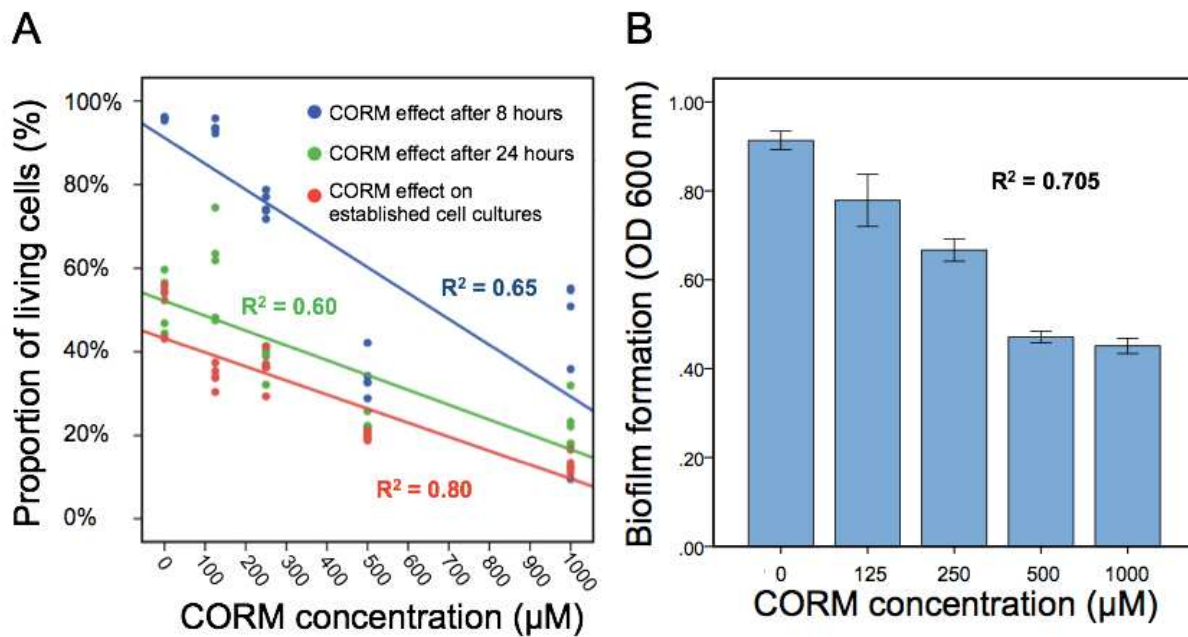
492 **FIGURES AND FIGURE LEGENDS**



493

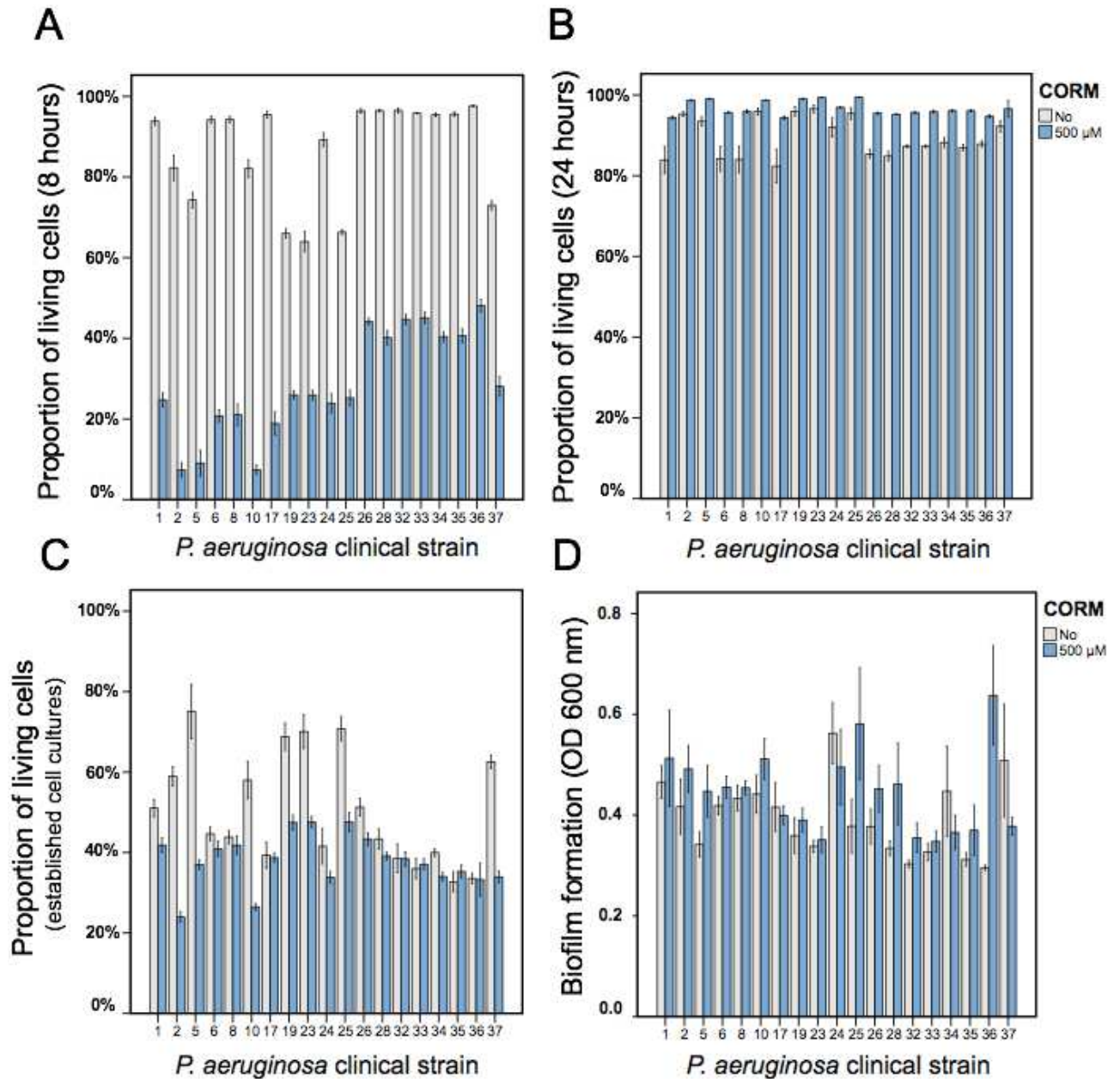
494 **Figure 1.** The stability of EBOR-CORM-1. Panel A shows the IR spectra of EBOR-CORM-
 495 1 upon heating at 50° C for 0 hours (black line), for 1 hours (red line), for 2 hours (blue) and
 496 for 3 hours (pink). The structure of the EBOR-CORM-1 is shown in inset on the left. Panel B
 497 shows the gas phase IR spectra of EBOR-CORM-1 in chloroform with added water where
 498 the * indicates a band from chloroform. Panel C shows the IR spectra of EBOR-CORM-1 in
 499 chloroform (top) and water (bottom) and panel D the IR spectra of CO in water after 1 min
 500 (top) and 90 min (bottom) dissolution. All frequencies given are in cm^{-1} .

501



502

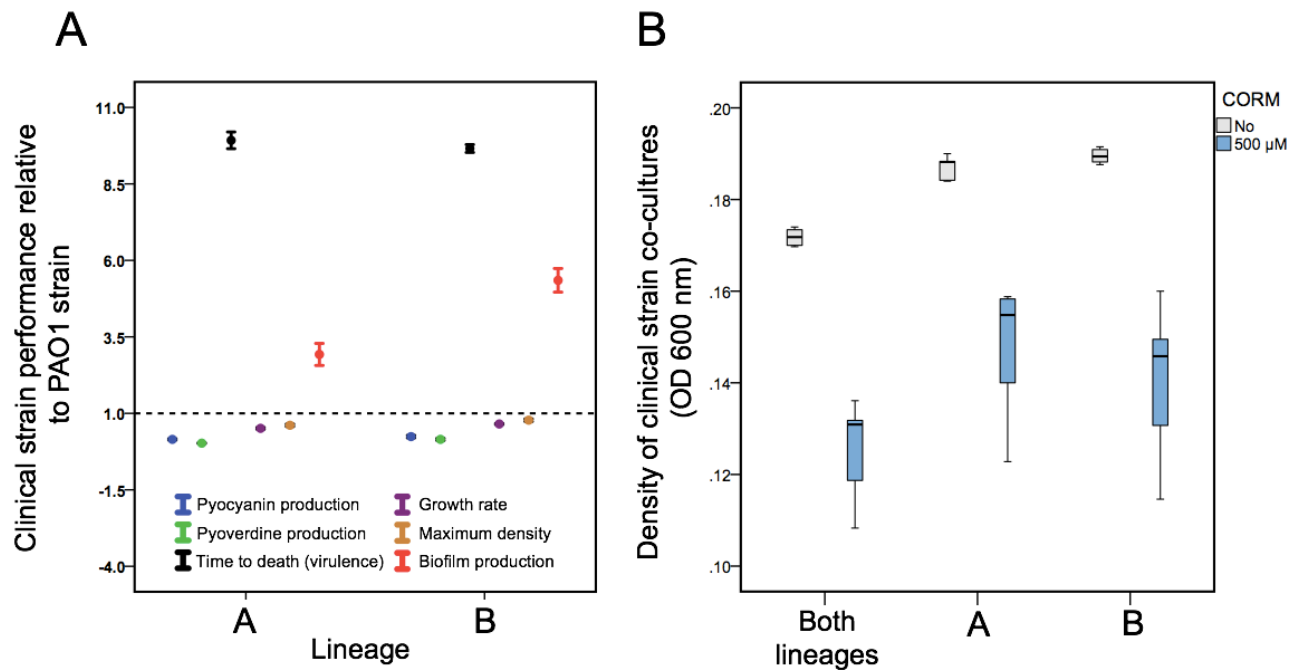
503 **Figure 2.** The EBOR-CORM-1 effects on planktonic and biofilm cells of *P. aeruginosa*
504 PAO1. In panel A, different lines denote for cell densities after 8 hours (blue line) and 24
505 hours (green line) of EBOR-CORM-1 application and EBOR-CORM-1 effects on established
506 cell cultures (red line) in different CORM concentrations. Panel B shows EBOR-CORM-1
507 effects on PAO1 biofilms in different CORM concentrations. The R^2 denotes for the fit of
508 regression with our data, and in panel B, bars denote for ± 1 s.e.m.



510

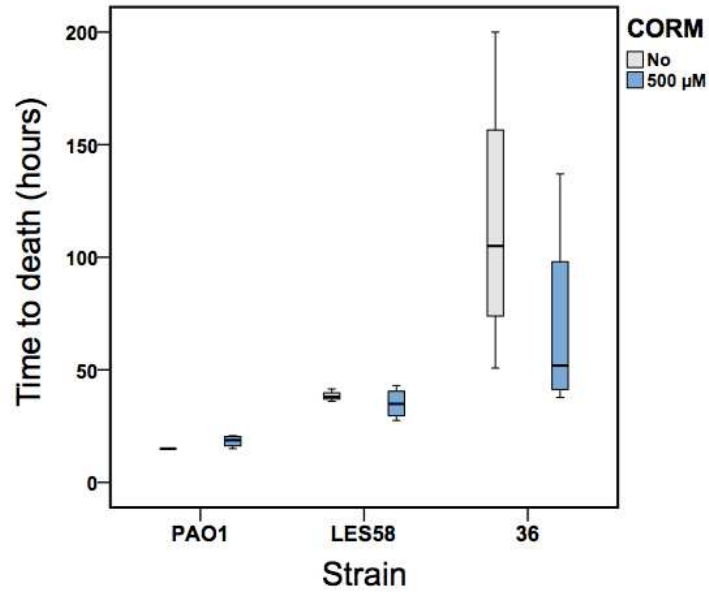
511 **Figure 3.** The EBOR-CORM-1 effects on planktonic and biofilm cells of clinical *P.*
 512 *aeruginosa* CF isolates. Panels A and B show the proportion of living cells after 8 hours and
 513 24 hours of EBOR-CORM-1 application, respectively. Panel C and D show the EBOR-
 514 CORM-1 effects on established cell cultures and biofilms, respectively. In all panels, bars
 515 denote for ± 1 s.e.m.

516



517
518

519 **Figure 4.** Differences in *P. aeruginosa* growth and virulence trait variation between PAO1
 520 and clinical CF isolates (panel A) and EBOR-CORM-1 effects on clinical CF isolate lineage
 521 mixes (panel B). In panel A, different colours denote for pyocyanin (blue) and pyoverdine
 522 (green) production, time to death (black), growth rate (purple), maximum density (yellow)
 523 and biofilm production for clinical isolates belonging to lineages A and B. The dashed line
 524 shows the mean performance of PAO1 strain. Panel B shows EBOR-CORM-1 effect on
 525 clinical CF isolate mixes after 24 hours of CORM application. In panel A, bars denote for ± 1
 526 s.e.m., and in panel B, extreme values around lower and upper quartile (black line shows the
 527 median).



528

529 **Figure 5.** The EBOR-CORM-1 activity against three *P. aeruginosa* strains in wax moth
 530 model. Boxplots show larval survival in the absence (light grey) and presence (blue) of
 531 EBOR-CORM-1 for PAO1, LESB58 and clinical isolate #36 (lineage B). Bars show extreme
 532 values around lower and upper quartile and black lines show the median.

533 **REFERENCES**

- 534 Angelici, R.J. (1964). Preparation, Characterization, and Reactions of the cis-
535 Dihalotetracarbonylmanganate (I) Anions. *Inorganic Chemistry* 3, 1099-1102.
- 536 Brown, E.D., and Wright, G.D. (2016). Antibacterial drug discovery in the resistance era.
537 *Nature* 529, 336-343.
- 538 Cochran, W., Mcfeters, G., and Stewart, P. (2000). Reduced susceptibility of thin
539 *Pseudomonas aeruginosa* biofilms to hydrogen peroxide and monochloramine.
540 *Journal of applied microbiology* 88, 22-30.
- 541 Cornforth, D.M., and Foster, K.R. (2013). Competition sensing: the social side of bacterial
542 stress responses. *Nature Reviews Microbiology* 11, 285-293.
- 543 De Beer, D., Stoodley, P., and Lewandowski, Z. (1997). Measurement of local diffusion
544 coefficients in biofilms by microinjection and confocal microscopy. *Biotechnology*
545 *and Bioengineering* 53, 151-158.
- 546 De Beer, D., Stoodley, P., Roe, F., and Lewandowski, Z. (1994). Effects of biofilm structures
547 on oxygen distribution and mass transport. *Biotechnology and bioengineering* 43,
548 1131-1138.
- 549 Desmard, M., Davidge, K.S., Bouvet, O., Morin, D., Roux, D., Foresti, R., Ricard, J.D.,
550 Denamur, E., Poole, R.K., Montravers, P., Motterlini, R., and Boczkowski, J. (2009).
551 A carbon monoxide-releasing molecule (CORM-3) exerts bactericidal activity against
552 *Pseudomonas aeruginosa* and improves survival in an animal model of bacteraemia.
553 *Faseb j* 23, 1023-1031.
- 554 El-Sayed, M., and Kaesz, H. (1963). Infrared Spectra and Structure of the Tetracarbonyl
555 Halide Dimers of Manganese, Technetium, and Rhenium. *Inorganic Chemistry* 2,
556 158-162.
- 557 Flume, P.A., Mogayzel, P.J., Robinson, K.A., Rosenblatt, R.L., Quittell, L., and Marshall,
558 B.C. (2010). Cystic Fibrosis Pulmonary Guidelines. *American Journal of Respiratory*
559 *and Critical Care Medicine* 182, 298-306.
- 560 Folkesson, A., Jelsbak, L., Yang, L., Johansen, H.K., Ciofu, O., Hoiby, N., and Molin, S.
561 (2012). Adaptation of *Pseudomonas aeruginosa* to the cystic fibrosis airway: an
562 evolutionary perspective. *Nature Reviews Microbiology* 10, 841-851.
- 563 Ghoul, M., West, S.A., Johansen, H.K., Molin, S., Harrison, O.B., Maiden, M.C., Jelsbak, L.,
564 Bruce, J.B., and Griffin, A.S. (2015). Bacteriocin-mediated competition in cystic
565 fibrosis lung infections. *Proc Biol Sci* 282.
- 566 Harrison, F., and Diggle, S.P. (2016). An ex vivo lung model to study bronchioles infected
567 with *Pseudomonas aeruginosa* biofilms. *Microbiology* 162, 1755-1760.
- 568 Harrison, F., Muruli, A., Higgins, S., and Diggle, S.P. (2014). Development of an ex vivo
569 porcine lung model for studying growth, virulence, and signaling of *Pseudomonas*
570 *aeruginosa*. *Infection and immunity* 82, 3312-3323.
- 571 Harrison, F., Paul, J., Massey, R.C., and Buckling, A. (2008). Interspecific competition and
572 siderophore-mediated cooperation in *Pseudomonas aeruginosa*. *ISME J* 2, 49-55.
- 573 Jimenez, J., Chakraborty, I., Carrington, S.J., and Mascharak, P.K. (2016). Light-triggered
574 CO delivery by a water-soluble and biocompatible manganese photoCORM. *Dalton*
575 *Trans* 45, 13204-13213.
- 576 Ketola, T., Mikonranta, L., Laakso, J., and Mappes, J. (2016). Different food sources elicit
577 fast changes to bacterial virulence. *Biol Lett* 12, 20150660.
- 578 Klein, M., Neugebauer, U., Gheisari, A., Malassa, A., Jazzazi, T.M., Froehlich, F.,
579 Westerhausen, M., Schmitt, M., and Popp, J.R. (2014). IR spectroscopic methods for
580 the investigation of the CO release from CORMs. *The Journal of Physical Chemistry*
581 *A* 118, 5381-5390.

582 Lu, S., Suharti, De Vries, S., and Moëne-Loccoz, P. (2004). Two CO Molecules Can Bind
583 Concomitantly at the Diiron Site of NO Reductase from *Bacillus a zotoformans*.
584 *Journal of the American Chemical Society* 126, 15332-15333.

585 Marvig, R.L., Johansen, H.K., Molin, S., and Jelsbak, L. (2013). Genome analysis of a
586 transmissible lineage of *Pseudomonas aeruginosa* reveals pathoadaptive mutations
587 and distinct evolutionary paths of hypermutators. *PLoS Genet* 9, e1003741.

588 Motterlini, R., and Otterbein, L.E. (2010). The therapeutic potential of carbon monoxide. *Nat*
589 *Rev Drug Discov* 9, 728-743.

590 Mowat, E., Paterson, S., Fothergill, J.L., Wright, E.A., Ledson, M.J., Walshaw, M.J.,
591 Brockhurst, M.A., and Winstanley, C. (2011). *Pseudomonas aeruginosa* population
592 diversity and turnover in cystic fibrosis chronic infections. *Am J Respir Crit Care*
593 *Med* 183, 1674-1679.

594 Murray, T.S., Okegbe, C., Gao, Y., Kazmierczak, B.I., Motterlini, R., Dietrich, L.E., and
595 Bruscia, E.M. (2012). The carbon monoxide releasing molecule CORM-2 attenuates
596 *Pseudomonas aeruginosa* biofilm formation. *PLoS One* 7, e35499.

597 Nobre, L.S., Seixas, J.D., Romao, C.C., and Saraiva, L.M. (2007). Antimicrobial action of
598 carbon monoxide-releasing compounds. *Antimicrob Agents Chemother* 51, 4303-
599 4307.

600 Normark, B.H., and Normark, S. (2002). Evolution and spread of antibiotic resistance.
601 *Journal of internal medicine* 252, 91-106.

602 O'brien, S., Williams, D., Fothergill, J.L., Paterson, S., Winstanley, C., and Brockhurst, M.A.
603 (2017). High virulence sub-populations in *Pseudomonas aeruginosa* long-term cystic
604 fibrosis airway infections. *BMC Microbiol* 17, 30.

605 O'neill, J. (2014). "Antimicrobial Resistance: Tackling a Crisis for the Health and Wealth of
606 Nations", in: *Review on Antimicrobial Resistance*. HM Government & Wellcome
607 Trust).

608 Poole, K. (2011). *Pseudomonas aeruginosa*: resistance to the max. *Front Microbiol* 2, 65.

609 Pritt, B., O'brien, L., and Winn, W. (2007). Mucoid *Pseudomonas* in cystic fibrosis. *Am J*
610 *Clin Pathol* 128, 32-34.

611 Reszka, K.J., O'malley, Y., McCormick, M.L., Denning, G.M., and Britigan, B.E. (2004).
612 Oxidation of pyocyanin, a cytotoxic product from *Pseudomonas aeruginosa*, by
613 microperoxidase 11 and hydrogen peroxide. *Free Radic Biol Med* 36, 1448-1459.

614 Rumbaugh, K.P., Trivedi, U., Watters, C., Burton-Chellew, M.N., Diggle, S.P., and West,
615 S.A. (2012). Kin selection, quorum sensing and virulence in pathogenic bacteria. *Proc*
616 *Biol Sci* 279, 3584-3588.

617 Smith, E.E., Buckley, D.G., Wu, Z., Saenphimmachak, C., Hoffman, L.R., D'argenio, D.A.,
618 Miller, S.I., Ramsey, B.W., Speert, D.P., Moskowitz, S.M., Burns, J.L., Kaul, R., and
619 Olson, M.V. (2006). Genetic adaptation by *Pseudomonas aeruginosa* to the airways of
620 cystic fibrosis patients. *Proceedings of the National Academy of Sciences of the*
621 *United States of America* 103, 8487-8492.

622 Stamellou, E., Storz, D., Botov, S., Ntasis, E., Wedel, J., Sollazzo, S., Kramer, B.K., Van
623 Son, W., Seelen, M., Schmalz, H.G., Schmidt, A., Hafner, M., and Yard, B.A. (2014).
624 Different design of enzyme-triggered CO-releasing molecules (ET-CORMs) reveals
625 quantitative differences in biological activities in terms of toxicity and inflammation.
626 *Redox Biol* 2, 739-748.

627 Stewart, P.S., and William Costerton, J. (2001). Antibiotic resistance of bacteria in biofilms.
628 *The Lancet* 358, 135-138.

629 Tinajero-Trejo, M., Rana, N., Nagel, C., Jesse, H.E., Smith, T.W., Wareham, L.K., Hippler,
630 M., Schatzschneider, U., and Poole, R.K. (2016). Antimicrobial Activity of the
631 Manganese Photoactivated Carbon Monoxide-Releasing Molecule [Mn (CO) 3 (tpa-
632 κ3 N)]+ Against a Pathogenic *Escherichia coli* that Causes Urinary Infections.
633 *Antioxidants & redox signaling* 24, 765-780.

634 Van Dommelen, S.M., Vader, P., Lakhal, S., Kooijmans, S., Van Solinge, W.W., Wood,
635 M.J., and Schiffelers, R.M. (2012). Microvesicles and exosomes: opportunities for
636 cell-derived membrane vesicles in drug delivery. *Journal of Controlled Release* 161,
637 635-644.

638 Ward, J.S., Lynam, J.M., Moir, J., and Fairlamb, I.J. (2014). Visible - Light - Induced CO
639 Release from a Therapeutically Viable Tryptophan - Derived Manganese (I)
640 Carbonyl (TryptoCORM) Exhibiting Potent Inhibition against E. coli. *Chemistry-A
641 European Journal* 20, 15061-15068.

642 Ward, J.S., Morgan, R., Lynam, J.M., Fairlamb, I.J., and Moir, J.W. (2017). Toxicity of
643 tryptophan manganese (I) carbonyl (Trypto-CORM), against *Neisseria gonorrhoeae*.
644 *MedChemComm* 8, 346-352.

645 Wareham, L.K., Poole, R.K., and Tinajero-Trejo, M. (2015). CO-releasing Metal Carbonyl
646 Compounds as Antimicrobial Agents in the Post-antibiotic Era. *J Biol Chem* 290,
647 18999-19007.

648 Wasser, I.M., Huang, H.-W., Moëne-Loccoz, P., and Karlin, K.D. (2005). Heme/non-heme
649 diiron (II) complexes and O₂, CO, and NO adducts as reduced and substrate-bound
650 models for the active site of bacterial nitric oxide reductase. *Journal of the American
651 Chemical Society* 127, 3310-3320.

652 Who.Int (2010). *WHO | Genes and human disease* [Online]. Available:
653 <http://www.who.int/genomics/public/geneticdiseases/en/index2.html> [Accessed 16-02
654 2017].

655 Williams, D., Evans, B., Haldenby, S., Walshaw, M.J., Brockhurst, M.A., Winstanley, C.,
656 and Paterson, S. (2015). Divergent, coexisting *Pseudomonas aeruginosa* lineages in
657 chronic cystic fibrosis lung infections. *Am J Respir Crit Care Med* 191, 775-785.

658 Williams, D., Paterson, S., Brockhurst, M.A., and Winstanley, C. (2016). Refined analyses
659 suggest that recombination is a minor source of genomic diversity in *Pseudomonas*
660 *aeruginosa* chronic cystic fibrosis infections. *Microbial Genomics* 2.

661 Wilson, J.L., Wareham, L.K., Mclean, S., Begg, R., Greaves, S., Mann, B.E., Sanguinetti, G.,
662 and Poole, R.K. (2015). CO-Releasing Molecules Have Nonheme Targets in Bacteria:
663 Transcriptomic, Mathematical Modeling and Biochemical Analyses of CORM-3
664 [Ru(CO)₃Cl(glycinate)] Actions on a Heme-Deficient Mutant of *Escherichia coli*.
665 *Antioxid Redox Signal* 23, 148-162.

666 Winstanley, C., Langille, M.G., Fothergill, J.L., Kukavica-Ibrulj, I., Paradis-Bleau, C.,
667 Sanschagrín, F., Thomson, N.R., Winsor, G.L., Quail, M.A., Lennard, N., Bignell, A.,
668 Clarke, L., Seeger, K., Saunders, D., Harris, D., Parkhill, J., Hancock, R.E.,
669 Brinkman, F.S., and Levesque, R.C. (2009). Newly introduced genomic prophage
670 islands are critical determinants of in vivo competitiveness in the Liverpool Epidemic
671 Strain of *Pseudomonas aeruginosa*. *Genome Res* 19, 12-23.

672 Winstanley, C., O'Brien, S., and Brockhurst, M.A. (2016). *Pseudomonas aeruginosa*
673 Evolutionary Adaptation and Diversification in Cystic Fibrosis Chronic Lung
674 Infections. *Trends Microbiol* 24, 327-337.

675 Workentine, M.L., Sibley, C.D., Glezerson, B., Purighalla, S., Norgaard-Gron, J.C., Parkins,
676 M.D., Rabin, H.R., and Surette, M.G. (2013). Phenotypic heterogeneity of
677 *Pseudomonas aeruginosa* populations in a cystic fibrosis patient. *PLoS One* 8, e60225.

678 Zhang, W.-Q., Atkin, A.J., Thatcher, R.J., Whitwood, A.C., Fairlamb, I.J., and Lynam, J.M.
679 (2009). Diversity and design of metal-based carbon monoxide-releasing molecules
680 (CO-RMs) in aqueous systems: revealing the essential trends. *Dalton Transactions*,
681 4351-4358.

682